ORGANIC LETTERS

2009
Vol. 11, No. 19
4326−4329

Synthesis, Crystal Structure, and Electron-Accepting Property of the BF_2 Complex of a Dihydroxydione with a Perfluorotetracene Skeleton

Katsuhiko Ono,*,† Junko Hashizume,† Hiroyuki Yamaguchi,† Masaaki Tomura,‡ Jun-ichi Nishida,§ and Yoshiro Yamashita§

Department of Materials Science and Engineering, Nagoya Institute of Technology, Gokiso, Showa-ku, Nagoya 466-8555, Japan, Institute for Molecular Science, Myodaiji, Okazaki 444-8585, Japan, and Department of Electronic Chemistry, Interdisciplinary Graduate School of Science and Engineering, Tokyo Institute of Technology, Nagatsuta, Midori-ku, Yokohama 226-8502, Japan

ono.katsuhiko@nitech.ac.jp

Received July 16, 2009

ABSTRACT

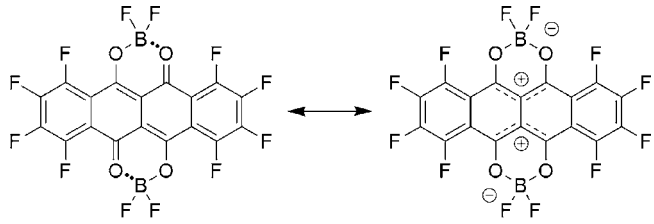

A BF_2 complex containing an octafluorotetracene moiety was synthesized as a new type of electron acceptor. This compound exhibits a long-wavelength absorption based on the perfluorotetracene skeleton and high electron affinity due to its quadrupolar structure enhanced by fluorination. In the crystal, the molecules are arranged with short F···π and F···F contacts affording a dense crystal packing. The BF_2 complex exhibited n-type semiconducting behavior.

Polycyclic aromatic compounds have attracted considerable attention since they are promising materials for active layers of organic field-effect transistors (OFETs).[1] Acene compounds such as pentacene and rubrene exhibit good p-type semiconducting properties.[2] These compounds have extended π-conjugation and rigid planality, thereby resulting in suitable intermolecular $\pi-\pi$ overlap and face-to-edge interactions in the solid state. On the other hand, n-type semiconductors with high electron affinities have been prepared by introduction of fluorine and trifluoromethyl groups into arene moieties as found in the synthesis of perfluoropentacene,[3] hexafluorohexa-*peri*-hexabenzocoronene[4] and 2,6-bis(4-trifluoro-

† Nagoya Institute of Technology.
‡ Institute for Molecular Science.
§ Tokyo Institute of Technology.

(1) (a) Murphy, A. R.; Fréchet, J. M. J. *Chem. Rev.* **2007**, *107*, 1066. (b) Zaumseil, J.; Sirringhaus, H. *Chem. Rev.* **2007**, *107*, 1296. (c) Anthony, J. E. *Chem. Rev.* **2006**, *106*, 5028. (d) Muccini, M. *Nat. Mater.* **2006**, *5*, 605. (e) Newman, C. R.; Frisbie, C. D.; da Silva Filho, D. A.; Brédas, J.-L.; Ewbank, P. C.; Mann, K. R. *Chem. Mater.* **2004**, *16*, 4436. (f) Bendikov, M.; Wudl, F.; Perepichka, D. F. *Chem. Rev.* **2004**, *104*, 4891.

(2) (a) Jurchescu, O. D.; Baas, J.; Palstra, T. T. M. *Appl. Phys. Lett.* **2004**, *84*, 3061. (b) Roberson, L. B.; Kowalik, J.; Tolbert, L. M.; Kloc, C.; Zeis, R.; Chi, X.; Fleming, R.; Wilkins, C. *J. Am. Chem. Soc.* **2005**, *127*, 3069. (c) Weidkamp, K. P.; Afzali, A.; Tromp, R. M.; Hamers, R. J. *J. Am. Chem. Soc.* **2004**, *126*, 12740. (d) Sundar, V. C.; Zaumseil, J.; Podzorov, V.; Menard, E.; Willett, R. L.; Someya, T.; Gershenson, M. E.; Rogers, J. A. *Science* **2004**, *303*, 1644. (e) Moon, H.; Zeis, R.; Borkent, E.-J.; Besnard, C.; Lovinger, A. J.; Siegrist, T.; Kloc, C.; Bao, Z. *J. Am. Chem. Soc.* **2004**, *126*, 15322. (f) Briseno, A. L.; Miao, Q.; Ling, M.-M.; Reese, C.; Meng, H.; Bao, Z.; Wudl, F. *J. Am. Chem. Soc.* **2006**, *128*, 15576. (g) Payne, M. M.; Parkin, S. R.; Anthony, J. E.; Kuo, C.-C.; Jackson, T. N. *J. Am. Chem. Soc.* **2005**, *127*, 4986. (h) Miao, Q.; Chi, X.; Xiao, S.; Zeis, R.; Lefenfeld, M.; Siegrist, T.; Steigerwald, M. L.; Nuckolls, C. *J. Am. Chem. Soc.* **2006**, *128*, 1340.

10.1021/ol901633q CCC: $40.75
Published on Web 08/27/2009

methylphenyl)anthracene.[5] Tetracarboxylic diimides with naphthalene,[6] anthracene,[7] and perylene[8] skeletons were also found to be good n-type semiconductors with high electron mobilities. Furthermore, electron-deficient heteropolycyclic compounds[9] and quinone derivatives[10] have been studied as potential electron-transporting materials. We recently synthesized BF_2 complexes of dihydroxydione of tetracene and perylene as a new type of electron-deficient arene compound.[11] The BF_2 chelation enhances the electron-withdrawing property as well as the π-electron delocalization of the tetracene and perylene moieties. Thus, these compounds showed long-wavelength absorptions and high electron affinity. The BF_2 complex with a tetracene skeleton (DHND−BF_2) exhibited n-type semiconducting behavior, although the electron mobility was not so high (1.5×10^{-5} $cm^2\ V^{-1}\ s^{-1}$). For improvement of its electron mobility, we undertook fluorination to DHND−BF_2 to yield a new electron acceptor F−DHND−BF_2 (Scheme 1). This compound is characterized by its quadrupolar structure enhanced by fluorination in its resonance contributor, affording small HOMO−LUMO energy and low-lying LUMO energy. The BF_2 chelation and fluorination also affect morphology in the molecular packing as heteroatom contacts. In this paper, we report the synthesis, electron-accepting properties, and crystal structure of F−DHND−BF_2 and its applications in the OFET study.

Scheme 1. Structure of BF_2 Complexes

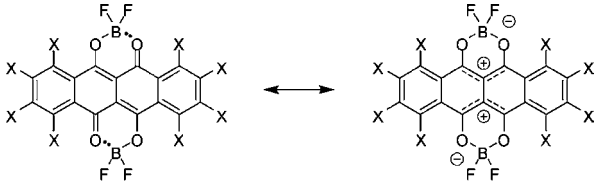

The synthesis of F−DHND−BF_2 was performed by chelation with boron trifluoride diethyl etherate (BF_3·OEt_2) to 1,2,3,4,7,8,9,10-octafluoro-6,11-dihydroxy-5,12-naphthacenedione (F−DHND), which was prepared with a synthetic method developed by Suzuki et al.[12] F−DHND−BF_2 was obtained as red crystals with a yield of 55% after sublimation at 275 °C under 10^{-3} Torr. This compound was stable in air in the solid state. However, it was more unstable in solution than DHND−BF_2 due to the ready hydrolysis. The thermogravimetric analysis (TGA) indicated a good thermal stability of F−DHND−BF_2. The 5% weight loss was observed at 277 °C, and this temperature is lower than that of DHND−BF_2 (325 °C). The weight loss is attributable to sublimation because a differential scanning calorimetry (DSC) analysis exhibited broad endothermic peaks in the region of 250−380 °C (Figure S9, Supporting Information).

The absorption and photoluminescence (PL) spectra of F−DHND−BF_2 in dichloromethane are shown in Figure 1a, and their spectroscopic properties are listed in Table 1. The absorption bands in the region of 430−580 nm are attributed to the tetracene moiety. These maxima are red-shifted as compared to those of DHND−BF_2. These red-shifts are due

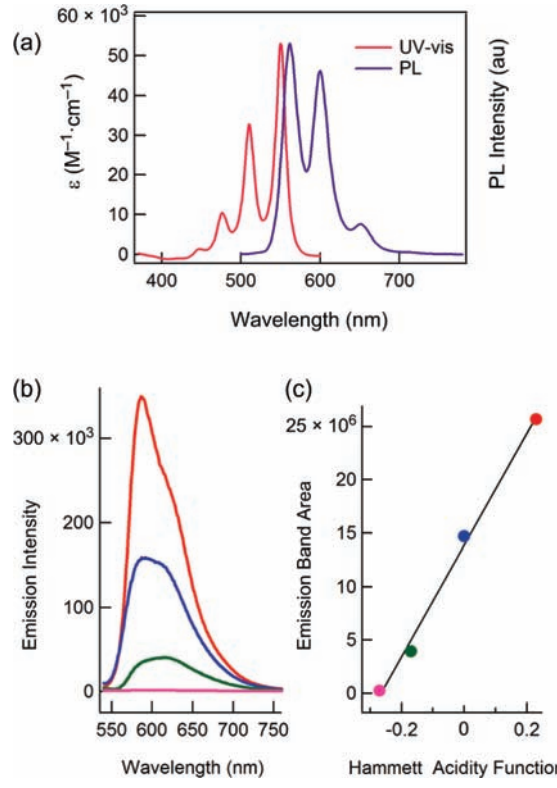

Figure 1. Spectroscopic properties of F−DHND−BF_2: (a) UV−vis and PL spectra in CH_2Cl_2, (b) PL spectra (concd 2.0×10^{-5} M) in aromatic solvents (red line, chlorobenzene; blue line, benzene; green line, toluene; pink line, anisole), and (c) relationship of emission band areas with Hammett acidity functions.

(3) Sakamoto, Y.; Suzuki, T.; Kobayashi, M.; Gao, Y.; Fukai, Y.; Inoue, Y.; Sato, F.; Tokito, S. *J. Am. Chem. Soc.* **2004**, *126*, 8138.

(4) Kikuzawa, Y.; Mori, T.; Takeuchi, H. *Org. Lett.* **2007**, *9*, 4817.

(5) Ando, S.; Nishida, J.; Fujiwara, E.; Tada, H.; Inoue, Y.; Tokito, S.; Yamashita, Y. *Chem. Mater.* **2005**, *17*, 1261.

(6) (a) Katz, H. E.; Lovinger, A. J.; Johnson, J.; Kloc, C.; Siegrist, T.; Li, W.; Lin, Y.-Y.; Dodabalapur, A. *Nature* **2000**, *404*, 478. (b) Katz, H. E.; Johnson, J.; Lovinger, A. J.; Li, W. *J. Am. Chem. Soc.* **2000**, *122*, 7787. (c) Jones, B. A.; Facchetti, A.; Marks, T. J.; Wasielewski, M. R. *Chem. Mater.* **2007**, *19*, 2703. (d) Babel, A.; Jenekhe, S. A. *J. Am. Chem. Soc.* **2003**, *125*, 13656.

(7) Wang, Z.; Kim, C.; Facchetti, A.; Marks, T. J. *J. Am. Chem. Soc.* **2007**, *129*, 13362.

(8) (a) Tatemichi, S.; Ichikawa, M.; Koyama, T.; Taniguchi, Y. *Appl. Phys. Lett.* **2006**, *89*, 112108. (b) Jones, B. A.; Facchetti, A.; Wasielewski, M. R.; Marks, T. J. *J. Am. Chem. Soc.* **2007**, *129*, 15259. (c) Jones, B. A.; Ahrens, M. J.; Yoon, M.-H.; Facchetti, A.; Marks, T. J.; Wasielewski, M. R. *Angew. Chem., Int. Ed.* **2004**, *43*, 6363.

(9) (a) Naraso; Nishida, J.; Kumaki, D.; Tokito, S.; Yamashita, Y. *J. Am. Chem. Soc.* **2006**, *128*, 9598. (b) Nishida, J.;Naraso; Murai, S.; Fujiwara, E.; Tada, H.; Tomura, M.; Yamashita, Y. *Org. Lett.* **2004**, *6*, 2007. (c) Nishida, J.; Murakami, S.; Tada, H.; Yamashita, Y. *Chem. Lett.* **2006**, *35*, 1236. (d) Tonzola, C. J.; Alam, M. M.; Kaminsky, W.; Jenekhe, S. A. *J. Am. Chem. Soc.* **2003**, *125*, 13548.

(10) (a) Mamada, M.; Nishida, J.; Tokito, S.; Yamashita, Y. *Chem. Commun.* **2009**, 2177. (b) Nishida, J.; Fujiwara, Y.; Yamashita, Y. *Org. Lett.* **2009**, *11*, 1813.

(11) Ono, K.; Yamaguchi, H.; Taga, K.; Saito, K.; Nishida, J.; Yamashita, Y. *Org. Lett.* **2009**, *11*, 149.

Table 1. Spectroscopic Properties of DHND Derivatives[a]

compound	λ_{abs} (nm)	λ_{PL} (nm)	λ_{edge} (eV)
F−DHND−BF_2	550, 510, 476	562, 600, 651	2.13
DHND−BF_2	523, 487, 455	529, 567, 615	2.23[b]
F−DHND	546, 508, 477	558, 595, 646 sh	2.14

[a] In CH_2Cl_2. [b] Reinvestigated.

to the introduction of fluorine atoms because their maxima are close to those of F−DHND. For F−DHND−BF_2, a small HOMO−LUMO energy gap of 2.13 eV was obtained from the absorption edge. The PL spectrum of F−DHND−BF_2 in dichloromethane exhibited a vibronic structure based on the tetracene moiety in the wavelength region of 530−680 nm. The Stokes shift is small (12 nm), indicating that F−DHND−BF_2 has a rigid geometry similar to that of DHND−BF_2 (6 nm). On the other hand, the PL spectrum of F−DHND−BF_2 in toluene is broad. The maximum (λ_{max} 615 nm) is red-shifted as compared to the shortest-wavelength maximum in dichloromethane. Figure 1b shows the PL spectra in various aromatic solvents in the concentration of 2.0×10^{-5} M. When the solvent with stronger electron-donating ability is used, the PL intensity decreases, where a linear relationship between their emission band areas and Hammett acidity functions of solvents is observed, as shown in Figure 1c. This quenching can be rationalized in terms of photoinduced charge-transfer interactions between F−DHND−BF_2 and electron-donating solvents, indicating the high electron affinity of F−DHND−BF_2.

To investigate the electron affinity of F−DHND−BF_2, the cyclic voltammetry (CV) measurement was performed in acetonitrile with 0.1 M *n*-Bu_4NClO_4. The voltammogram displays two reversible reduction waves, as shown in Figure 2. The half-wave reduction potentials of F−DHND−BF_2 are

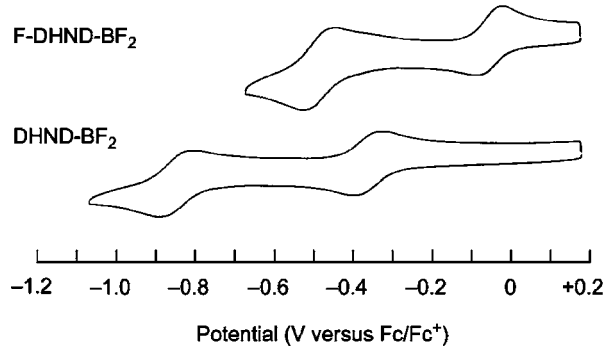

Figure 2. Cyclic voltammograms of BF_2 complexes.

observed at −0.06 and −0.50 V versus Fc/Fc^+. These values are more positive than those of DHND−BF_2 ($E_{1/2}^{red}$: −0.37 and −0.85 V), indicating an increase of electron affinity by fluorination to the DHND skeleton. These reduction potentials are more positive than those of F−DHND (E_p^{red}: −0.91 V) and perfluorotetracene (F−tetracene) (E^{red}: −1.49 V).[12] Therefore, the electron-accepting ability of F−DHND−BF_2 is much greater than those of F−DHND and F−tetracene. This result is attributed to the BF_2 chelation, which yields the quadrupolar resonance structure (Scheme 1). The difference between the first and second reduction potentials for F−DHND−BF_2 (0.44 V) is smaller than that for DHND−BF_2 (0.48 V), indicating that on-site Coulomb repulsion is slightly decreased by the fluorination.

The molecular structure of F−DHND−BF_2 was investigated by X-ray crystallographic analysis. Single crystals suitable for the X-ray analysis were grown by slow sublimation. In the crystal, the molecule is centrosymmetric, as shown in Figure 3a. The two boron atoms exist on the center

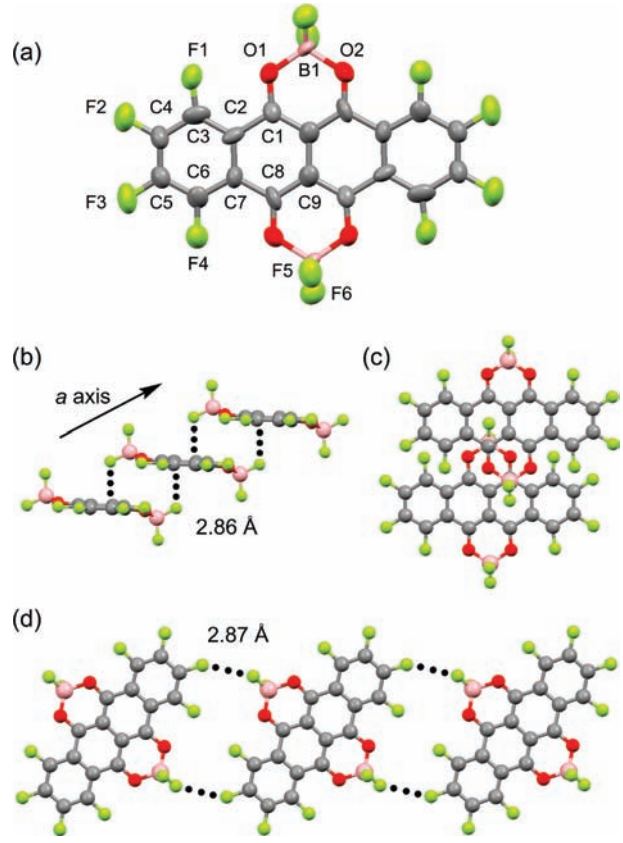

Figure 3. Crystal structure of F−DHND−BF_2: (a) molecular structure (ellipsoid); (b) molecular stacking; (c) overlap mode; (d) molecular tape.

line of the molecule, and the B_1-O_1 and B_1-O_2 bond distances are 1.48(1) and 1.52(1) Å, respectively. The tetracene moiety is planar. The B−F bonds are asymmetrically placed on the molecular plane (Figure 3b), and the B_1-F_5 and B_1-F_6 bonds are 1.37(1) and 1.35(1) Å, respectively. The molecules are stacked along the *a* axis to form a column with short F···π contacts. The fluorine atoms

(12) Sakamoto, Y.; Suzuki, T.; Kobayashi, M.; Gao, Y.; Inoue, Y.; Tokito, S. *Mol. Cryst. Liq. Cryst.* **2006**, *444*, 225.

are interacted with the benzene rings of the neighboring molecules with an intermolecular distance of 2.86 Å (Figure 3c). This contact distance is shorter than the sum of the van der Waals radii of fluorine and carbon atoms (3.17 Å). The molecules are arranged to form a molecular tape with short F···F contacts, whose contact distances are 2.87 Å (Figure 3d). These heteroatom contacts lead to a dense crystal packing (D_x = 2.10 g cm^{-3}).

The molecular orbital (MO) calculations of F−DHND−BF_2 and its related compounds were performed using B3LYP/6-31G(d),[13] and the energy diagram of their HOMOs and LUMOs is summarized in Figure 4. Although

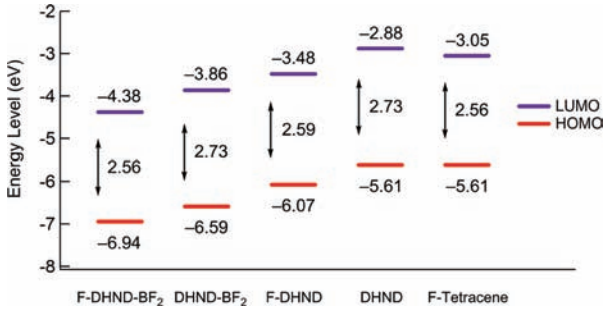

Figure 4. Energy diagram of the HOMOs and LUMOs of F−DHND−BF_2 and its related compounds obtained by B3LYP/6-31G(d) calculations.

both the BF_2 chelation and fluorination work for a decrease of their HOMO and LUMO energies, the BF_2 chelation is more effective since the HOMO and LUMO energies of BF_2 complexes are lower than those of F−tetracene. Furthermore, the small HOMO−LUMO energy gap of F−DHND−BF_2 is attributable to the F−tetracene skeleton, where the orbitals in the HOMO and LUMO are extended on the fluorine groups. These calculations are consistent with the CV data and UV−vis absorption spectra of F−DHND−BF_2 and its related compounds.

The field-effect mobilities were measured on the devices with a bottom contact configuration. The organic layers were fabricated on an SiO_2 dielectric layer by vacuum deposition (10^{-5} Pa), and the OFET measurements were performed in a vacuum. The films of F−DHND−BF_2 exhibited n-type semiconducting behavior (Figure S12, Supporting Information), and the characteristics of OFET devices are listed in Table 2. Both the treatment of the substrate surface with hexamethyldisilazane (HMDS) and the substrate temperature are effective for increases of its electron mobility and on/off ratio. According to the X-ray diffraction (XRD) analysis, the film deposited on the HMDS surface at 65 °C exhibits three diffraction peaks (*d* space values: 10.39, 5.19, and 3.47 Å), whereas the films deposited at room temperature do not show any XRD peaks (Figure S13, Supporting Information). This fact indicates that the crystallinity of films increased by annealing. The *d*-spacing of 10.39 Å suggests that the molecules stand with the BF_2 units on the substrate affording a layer structure. The field-effect mobilities may be attributed to this molecular aggregation. The threshold voltages observed are relatively small, indicating effective electron injection due to the high electron-accepting property of F−DHND−BF_2.

(13) See Supporting Information for the MO calculations.

Table 2. OFET Performance of F−DHND−BF_2 Films

surface	substrate temp (°C)	mobility (cm^2/V·s)	on/off ratio	threshold (V)
bare	rt	9.1×10^{-7}	2×10^2	+5
HMDS	rt	2.6×10^{-5}	3×10^4	+17
HMDS	65	7.8×10^{-5}	4×10^5	+14

In conclusion, we synthesized a BF_2 complex with an octafluorotetracene moiety as a new type of electron acceptor. This compound exhibited a small HOMO−LUMO energy gap and a high electron affinity, as observed from the spectral and electrochemical studies. The small HOMO−LUMO energy gap is attributable to the F−tetracene skeleton. Both the BF_2 chelation and fluorination are highly effective for a decrease of LUMO energy. In the crystal, the molecules are arranged to form a tapelike network with short F···π and F···F contacts, leading to a dense crystal packing. The BF_2 complex showed n-type semiconducting behaviors in the devices with a bottom contact configuration. Further investigation on the OFET application of F−DHND−BF_2 is in progress.

Acknowledgment. This work was supported by a Grant-in-Aid for Scientific Research (No. 20550037) from the Ministry of Education, Culture, Sports, Science and Technology, Japan. We thank ADEKA CORP. for their financial support. We also thank Prof. T. Suzuki (Institute for Molecular Science) for his kind help for the synthesis of F−DHND and the Instrument Center of the Institute for Molecular Science for the X-ray structure analyses.

Supporting Information Available: Synthetic procedures, additional characterization data, and X-ray crystallographic data in CIF format. This material is available free of charge via the Internet at http://pubs.acs.org.

OL901633Q